The Birth and Death Process of Hypercycle Spirals

Kazumasa Oida
ATR Adaptive Communications Research Laboratories
2-2-2 Hikaridai Seika-cho Soraku-gun Kyoto 619-0288 Japan
oida@atr.co.jp

Abstract

The behavior of hypercycle spirals in a two-dimensional cellular automaton model is analyzed. Each of these spirals can be approximated by an Archimedean spiral and the center, width, and phase of the hypercycle spiral change according to Brownian motion. A barrier exists between two spirals if the phase synchronization hypothesis is taken into account, and the occurrence rate of pair decay (the simultaneous disappearance of two spirals) can be explained by the random walk simulation with the barrier. Adjacent species violation is shown to be a necessary condition for creating new spirals. A hypercycle system can live long if the spirals in the system are somewhat unstable, since new spirals cannot emerge when existing spirals are too stable.

Introduction

A hypercycle, as introduced by Eigen (Eigen 1971) in 1971, is a system that consists of a number of self-replicative molecular species that are linked cyclically by catalysis (Fig. 1). The idea of the hypercycle is important in the study of pre-biotic evolution because it may explain how molecular species having a small number of molecules can evolve into an entity with a great amount of genetic information. Since Eigen's initial work, hypercycles have been experimentally and theoretically verified (Gebinoga 1995). In particular, the stability of hypercycles has been extensively studied in terms of nonlinear ordinary differential equations (ODE) (Eigen & Schuster 1979; Hofbauer & Sigmund 1988). The results from ODEs have indicated that hypercycles are not always stable systems; they tend to be vulnerable to parasites. ODEs, however, do not take into account any spatial effects among molecules.

In 1991, Boerlijst and Hogeweg (Boerlijst & Hogeweg 1991; 1992) were the first to show the spatial dynamics caused by hypercyclic interactions; "spiral waves" emerged in their cellular automaton (CA) model and, interestingly, the spirals made the hypercycles resistant to parasites. In 1995, Cronhjort and Blomberg (Cronhjort & Blomberg 1996) considered a more realistic case, i.e., the maximum concentration (c_0) of all molecules is limited (growth limitation), and reported that hypercycles with a few components, which do not exhibit spiral waves but homogeneous clusters, are also resistant to parasites. In 1995, Vespalcova et al. (Vespalcova, Holden, & Brindley 1995) introduced inhibitory connections into the hypercycle structure and found that, under some circumstances, these connections enhance the resistance to parasites. In 1998, Altmeyer et al. (Altmeyer, Wilke, & Martinetz 1998) reported that hypercycle interactions generate rotating screws and corn-like structures in their three-dimensional CA model.

As mentioned above, previous works have mainly focused on how hypercycle systems can coexist with parasites. In contrast, this paper focuses on a more basic question: how do spirals in a two-dimensional CA model appear and disappear? The birth and death mechanism of hypercycle spirals, which should provide important information on the stability of hypercycles, is currently unclear. Our model is similar to the Cronhjort model (a two-dimensional CA model under growth limitation). However, it has six species, so that spirals emerge.

To understand the mechanism, we follow the behavior of spirals in an analytic way. We show quantitatively that the shape of a spiral can be approximated by an Archimedean spiral and that its center, width, and phase change according to Brownian motion. Then, we show the impact of c_0 and the decay probability of a molecular species (P_{decay}) on the birth and death process of hypercycle spirals. Parameter space (c_0, P_{decay}) can be divided into three regions: systematic (S), quasi-systematic (Q), and chaotic (C) regions. In the S region, the number of spirals monotonically decreases with time due to pair decay (the simultaneous disappearance of two spirals), which was first mentioned by Boerlijst and Hogeweg (Boerlijst & Hogeweg 1991). In the Q region, not only is there pair decay, but also independent decay. New spirals may emerge after the occurrence of an independent decay. In the C region, spirals do not form.

Next, we explain how two spirals interact based on the phase synchronization hypothesis, which states that two spirals are in contact with each other such that molecules of the same species meet at the boundary between these

spirals. This hypothesis yields a barrier between spirals. The shape of the barrier depends on the spirals' rotation directions and affects the occurrence rate of pair decay. We then introduce the term "adjacent species violation (ASV)," which represents a phenomenon in which a belt of species i touches a belt made up of species other than $i-1$, i, and $i+1$, where a spiral is composed of six belts and each belt is made up of molecules of the same species. We show from computational experiments that ASV is a necessary condition for creating new spirals. Lastly, we show that in order for a hypercycle system to live long, spirals in the system must be somewhat unstable, since new spirals cannot emerge when existing spirals are too stable.

The CA Model

In order to model a reaction-diffusion system of six molecular species in a hypercycle organization (in Fig. 1) in a two-dimensional medium, we consider a two-dimensional cellular automaton (CA) model, which is on a 200×200 lattice of square cells with periodic boundaries. Let s_k be the state of a cell k. Cell k is either occupied by a molecule of species i (i.e., $s_k = i$) or empty (i.e., $s_k = 0$). Hereafter, we call the states of all cells on the lattice an image. The CA starts at $t = 0$ with an image consisting of $200^2 c_0$ molecules, whose species and positions are randomly selected according to a uniform distribution. c_0 is a parameter indicating the maximum total concentration ($0 < c_0 \leq 1$).

We explain our model concisely since it is mostly derived from the Boerlijst and Cronhjort models (Boerlijst & Hogeweg 1991; 1992; Cronhjort & Blomberg 1996). At each time step, for all cells k (200^2 in total), s_k is updated in random order as follows:

if $(s_k = 0)$
  for each $i \in S_i$ **do**
    $P_i := (1 - \frac{c_{\rm tot}}{c_0}) \frac{\rm support}(i)}{\max(\sum_{i \in S_i} {\rm support}(i), \alpha)}$;
  if $(\sum_{j=1}^{i-1} P_j < X_1 \leq \sum_{j=1}^{i} P_j)$
    $s_k := i$;
    $c_{\rm tot} := c_{\rm tot} + \frac{1}{200^2}$;
else
  if $(X_2 \leq P_{\rm decay})$
    $s_k := 0$;
    $c_{\rm tot} := c_{\rm tot} - \frac{1}{200^2}$;
  else $(X_3 \leq P_{\rm diff})$
    diffuse(k);

In the above algorithm, S_i ($= \{1,2,3,4,5,6\}$) is the set of species in the hypercycle (Fig. 1). X_1, X_2, and X_3 represent random numbers generated according to the uniform distribution in range [0,1]. Function diffuse(k) interchanges s_k with s_j, where j is a randomly selected neighboring cell of k. Throughout this paper, a neighboring cell of cell k is one of eight cells surrounding cell k (Moore neighborhood).

P_i in the algorithm denotes the probability that a molecule of species i is replicated into cell k. To obtain probability P_i, we first calculate the amount of replication support for species i at cell k such that

$$\text{support}(i) = N_i \text{self}(i) + N_{i,i-1} \text{cat}(i, i-1),$$

where N_i is the number of k's neighboring cells that are occupied by species i. $N_{i,j}$ is the number of pairs of cells ℓ and m that satisfies three conditions: $\ell, m \in$ {neighboring cells of cell k}, $(s_\ell, s_m) = (i,j)$ or (j,i), and ℓ is a neighbor of m. Functions self(i) and cat(i,j) represent relative replication rates of species i by self-replication and by replication with catalytic support from j, respectively.

In the same way as in the Cronhjort model (Cronhjort & Blomberg 1996), we introduce the growth limiting factor $\gamma = 1 - c_{\rm tot}/c_0$, where $c_{\rm tot}$ is the fraction of cells occupied by any molecule. We introduce the growth limitation to observe the effect of the amount of components used for building up molecules. When $\gamma \approx 0$ (i.e., $c_0 \approx c_{\rm tot}$), all replication probabilities are almost zero; therefore, the growth stops under such a condition. Parameter α controls the probability that one molecule of any species is replicated into an empty cell. If α increases, the probability decreases, so that replications occur only at empty cells having large R values, where $R = \sum_{i \in S_i} \text{support}(i)$. Therefore, $c_{\rm tot}$ decreases as α increases. A molecule decays with probability $P_{\rm decay}$. All parameter values in this model except for c_0 and $P_{\rm decay}$ are shown in Table 1.

The following summarizes the characteristics of our model. (1) The states of all cells are asynchronously updated at each time step. (2) The replication probability of species i is larger than that of species j if support(i) > support(j). (3) Growth limitation is taken into account. (4) Parameter α controls the replication probability at all empty cells.

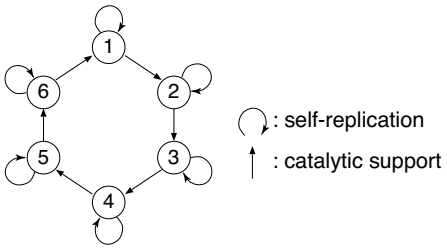

Figure 1: A hypercycle consisting of six species.

Table 1: Parameter values used to obtain all results in this paper, unless stated otherwise.

self(i)	0.01 for all $i \in S_i$
cat($i, i-1$)	1 for all $i \in S_i$
α	1
$P_{\rm diff}$	0.5

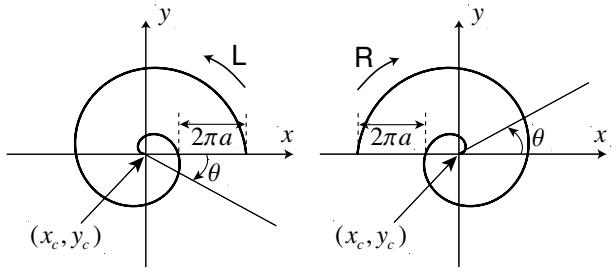

Figure 2: θ advancing in the opposite direction against the rotation direction of a spiral.

Dynamics of Hypercycle Spirals

In this section, we first explain analytically the shape and movement of an individual spiral, and then describe the effects of c_0 and $P_{\rm decay}$ on the dynamics of spirals, especially on their birth and death process.

Archimedean Spiral

A spiral consists of six belts, each of which is made up of molecules of the same species. Although the boundary between two belts is not smooth, it can be approximated by an Archimedean spiral (see Fig. 12(a)) with our spiral identification method. This result is the starting point of our work. Based on this result, the boundary between belts of species i and $i-1$ can be written with orthogonal coordinates (x, y) as

$$x = x_c + a\theta\cos(\theta - \frac{2\pi}{6}i + \varphi), \quad (1)$$

$$y = y_c \pm a\theta\sin(\theta - \frac{2\pi}{6}i + \varphi), \quad (2)$$

where (x_c, y_c), φ, and a are, respectively, the center, phase, and width of the spiral, and $0 \le \theta \le 2n\pi$ when the number of turns is n. Each spiral has its own rotation direction, which is either clockwise (R) or counterclockwise (L). As shown in Fig. 2, θ advances in the opposite direction against the rotation direction. Therefore, the second term on the right-hand side of Eq. (2) takes the positive (negative) sign if the rotation direction is R (L).

We obtained time series of center $(x_c(t),\ y_c(t))$, phase $\varphi(t)$, and width $a(t)$ of a spiral from about 6000 images. Figure 3 shows the case of $(c_0, P_{\rm decay}) = (0.2, 0.04)$; the case of $(c_0, P_{\rm decay}) = (0.7, 0.06)$ is almost the same. Let

$$\dot{x}_c(k) = x_c(t+k) - x_c(t), \quad \dot{\varphi}(k) = \varphi(t+k) - \varphi(t),$$
$$\dot{y}_c(k) = y_c(t+k) - y_c(t), \quad \dot{a}(k) = a(t+k) - a(t).$$

We can see that histograms of the four increments $(\dot{x}_c(k), \dot{y}_c(k), \dot{\varphi}(k), \dot{a}(k))$ approximate normal distributions. Figure 3(b) shows the histogram of $\dot{\varphi}(k)$. In the figure, $N(\mu, \sigma^2)$ indicates a normal distribution with mean μ and variance σ^2. Furthermore, as shown in Fig. 3(c), the sample standard deviations of the four increments linearly increase with $\sqrt{k}$ for large k's; therefore, their behavior can be regarded approximately as Brownian motion. (However, we show exceptions later.) The absolute value of the correlation coefficient between any two increments is almost zero (less than 1.5×10^{-3} when $(c_0, P_{\rm decay}) = (0.2, 0.04)$) except for that between $\dot{\varphi}(t)$ and $\dot{a}(t)$ (its maximum is 0.0216 when $(c_0, P_{\rm decay}) = (0.2, 0.04)$).

Figure 3(a) shows a random walk of a spiral's center $(x_c(t),\ y_c(t))$. Its movement is perceptible to the naked eye. The angular frequency $\omega (= \dot{\varphi}(1))$ of a spiral is almost constant, since its variance is very small. The rotation time $T_r = 2\pi/\bar{\omega}$ agrees with that computed by Boerlijst's method (Boerlijst & Hogeweg 1992), where $\bar{\omega}$ is the sample mean of ω. T_r decreases with an increase in $P_{\rm decay}$. For many c_0 and $P_{\rm decay}$ pairs, their relation is roughly $T_r P_{\rm decay} \approx 130$. The sample mean of width a also decreases with an increase in $P_{\rm decay}$.

Parameter Space

Based on the behavior of spirals, parameter space $(c_0, P_{\rm decay})$ is divided into three regions: systematic (S), quasi-systematic (Q), and chaotic (C) regions (Fig. 4). The Q region is made up of Q1 and Q2 sub-regions. In the S region, all spirals die out due to pair decay (see Figs. 12(d)-(f)). A pair decay is the simultaneous disappearance of two spirals and occurs when the distance between their centers becomes very short. A pair decay occurs only if the rotation directions of two spirals are different. As shown in Fig. 5, the number of spirals in this region is always an even number and the number gradually decreases two by two with time, until it eventually becomes zero.

In the Q region, not only pair decay, but also independent decay can be observed. An independent decay is the collapse of a spiral caused by the intensive decay of molecules in the spiral. If such intensive decay occurs at the center of a spiral, before long the spiral disappears (this type of independent decay is called a complete decay); otherwise it survives (this is called a partial decay). New spirals are often born just after a partial decay. Accordingly, the number of spirals decreases after a pair or a complete decay, but it may increase after a partial decay (Fig. 5).

In the S region, spirals cover the whole square lattice. In the Q1 region, on the other hand, a few masses of empty cells exist between spirals (they look like lakes on a continent, as shown in Fig. 12(b)), while in the Q2 region, a few spirals are surrounded by empty cells (they look like islands, as shown in Fig. 12(c)).

In the C region, molecules cannot form spirals, so all molecules die out shortly after the model starts. There are some reasons why they cannot form spirals. For example, if $P_{\rm decay}$ is very large, the life spans of the molecules become too short to form spirals, while if $P_{\rm decay}$ is very small, the width a of a spiral becomes too large to form spirals on the 200×200 lattice.

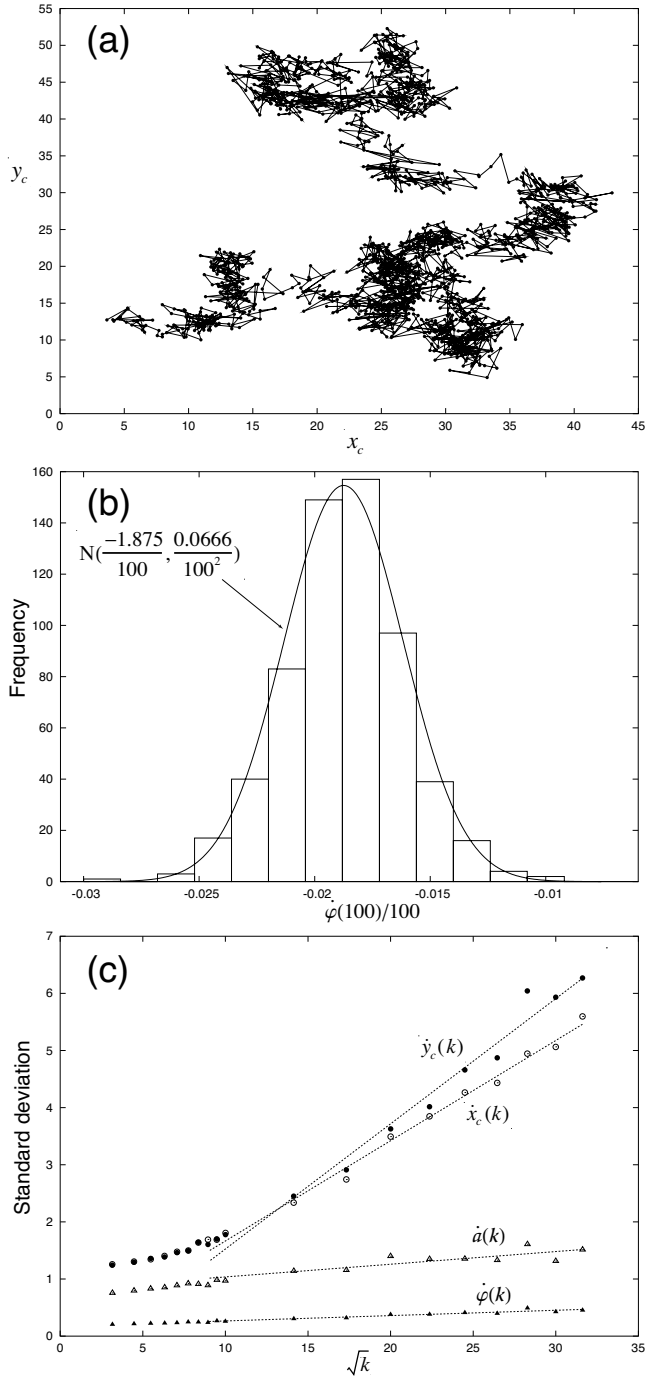

Figure 3: Behavior of a spiral derived from 6116 images when $(c_0, P_{\text{decay}}) = (0.2, 0.04)$. (a) Random walk of center $(x_c(t), y_c(t))$. (b) A histogram of $\dot{\varphi}(100)/100$ (radian/time-step), where the cell size is 1.6×10^{-3} radians. (c) Standard deviations increasing linearly with $\sqrt{k}$.

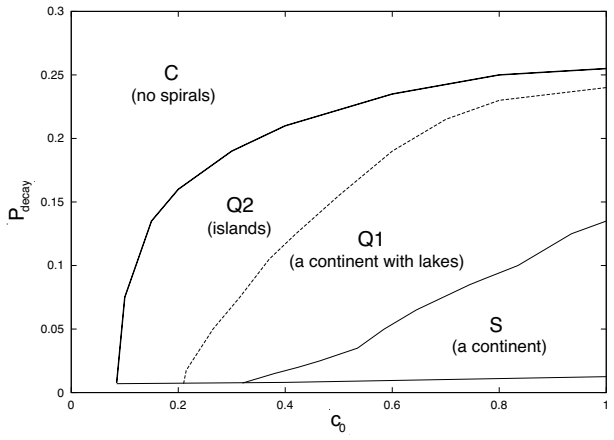

Figure 4: Regions in parameter space (c_0, P_{decay}).

Phase Synchronization

Hypothesis

The CA lattice can be divided into n areas when there are n spirals in an image. One Archimedean spiral exists in each area and the shape of each area gradually changes with time. Two belts belonging to different spirals meet at a boundary of two areas (for example, see Fig. 7). At each point on the boundary, six belts composed of different species cyclically arrive from both areas. We have noticed that two belts meeting on the boundary are always made up of the same species. We call such a state of two spirals "phase synchronization" and establish the following hypothesis.

Phase synchronization hypothesis: All spirals that are in contact with one another are in the phase synchronization state if no partial decays are in progress.

If the hypothesis is true, a belt of species i is always enclosed only by belts of species $i-1$, i, and $i+1$. This hypothesis is very natural since species i is created at an empty cell next to species $i-1$ (with the catalytic support of $i-1$) or next to species i (by self-replication). Note that this hypothesis states that the phase synchronization holds even though complete or pair decays are in progress. The progress of these decays is such that a mass of empty cells expands outward from the center until it reaches area boundaries (see Fig. 12(f)); therefore, the hypothesis holds even during these decays.

We use the hypothesis as a basis to explain the following facts:

- A pair decay occurs only if the rotation directions of two spirals are different.
- If the distance between the centers of two spirals rotating in the same direction becomes very short, they repel each other.

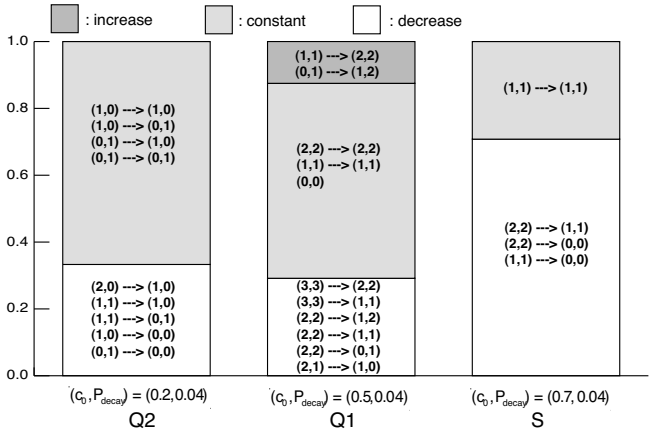

Figure 5: Probabilities that the number of spirals increases, decreases, and remains unchanged between $t = 10^4$ and $t = 10^5$ in three regions (Q1, Q2, S). The number of trials is 24. The patterns of changes are described as "(L_1, R_1)—> (L_2, R_2)," where L_1 (R_1) and L_2 (R_2) are numbers of spirals rotating clockwise (counterclockwise) observed at $t = 10^4$ and $t = 10^5$, respectively.

Barrier between Spirals

We first show how close two spirals can come to each other while maintaining the phase synchronization state. Here, we express the four parameters (x_c, y_c, φ, a) of Archimedean spiral i as $(x_i, y_i, \varphi_i, a_i)$. Let d be the distance between the centers of two spirals and let S_d denote the range of distances d that do not allow two spirals to be in the phase synchronization state. Figure 6 shows range S_d as a function of phase difference ($\Delta\varphi = \varphi_2 - \varphi_1$) obtained with Eqs. (1) and (2) under the condition that $y_1 = y_2 = 0$ and $a_1 = a_2 = a$. We computed the boundary between two spirals since if their complete boundary can be obtained, they are in the synchronization state. As shown in the figure, spirals with different directions can come closer to each other than spirals with the same direction. Let d_s be the greatest lower bound in the complementary range of S_d ($\bar{S}_d$). When the directions are different, there are no S_d barriers ($d_s = 0$) between them if $\Delta\varphi \approx \pi$; however, since the gap in the barrier is extremely narrow (less than 10^{-5} radians) when $d < 1.97a$, it may be difficult to enter the gap. Meanwhile, if the rotation directions are the same, $d_s \approx 3.107a$ when $\Delta\varphi = \pi$.

We next show the reason why the pair decay occurs. The direct cause of pair or complete decay is that at least one of the six belts disappears from the center of the spiral. Figure 7 shows two spirals with different rotation directions, which are depicted according to Eqs. (1) and (2). As shown in the figure, if distance d is very small, a belt with a small area appears (belt 1 in Fig. 7). Since two spirals with different rotation directions can come very close to each other, the chance of a belt disappearing (due to an intensive decay of molecules in the belt) is large. Figure 12(e) shows two spirals in our CA model whose shapes are similar to those in Fig. 7. Contrarily, if their directions are the same, such a small area does not appear even if $d = d_s$.

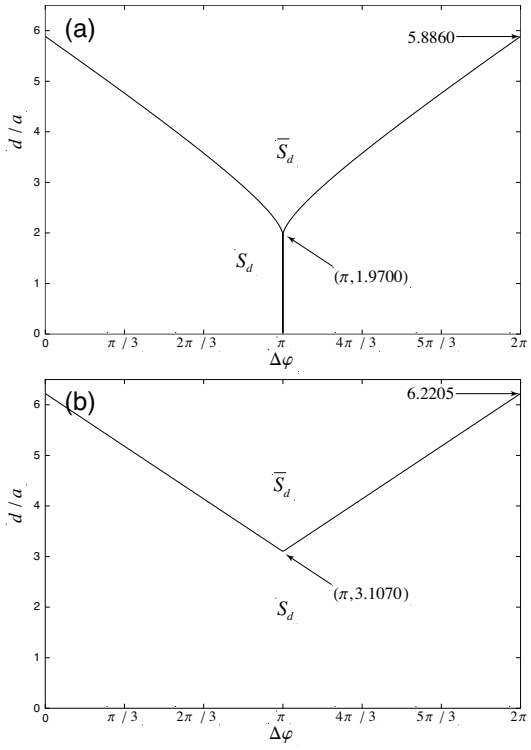

Figure 6: Range S_d of distances that do not allow two spirals to be in the phase synchronization state when rotation directions are (a) different and (b) the same.

Phase Difference

The phase difference between two spirals is a relative quantity; therefore, it should be an invariant with respect to the translation and rotation of the coordinate axes. In the previous section, we dealt with the case $y_1 = y_2$, and expressed the phase difference as $\Delta\varphi = \varphi_2 - \varphi_1$. In this section, we assume that $y_1 \neq y_2$.

We first consider the case where the rotation directions of two spirals are different. Suppose the center of spiral 2 in Fig. 8 moves from (x_2, y_1) to (x_2, y_2) while its phase φ_2 remains unchanged. After the movement, by observing spiral 1 from spiral 2 (in other words, by regarding the line that passes points (x_1, y_1) and (x_2, y_2) as the X-axis), the phase of spiral 1 (φ_1) decreases by $\phi = \tan^{-1}\frac{y_2 - y_1}{x_2 - x_1}$ $(-\pi \leq \phi \leq \pi)$, where

$$\begin{cases} 0 \leq \phi \leq \frac{\pi}{2}, & \text{if } x_2 - x_1 \geq 0 \text{ and } y_2 - y_1 \geq 0, \\ \frac{\pi}{2} < \phi \leq \pi, & \text{if } x_2 - x_1 < 0 \text{ and } y_2 - y_1 \geq 0, \\ -\frac{\pi}{2} \leq \phi < 0, & \text{if } x_2 - x_1 \geq 0 \text{ and } y_2 - y_1 < 0, \\ -\pi < \phi < -\frac{\pi}{2}, & \text{if } x_2 - x_1 < 0 \text{ and } y_2 - y_1 < 0. \end{cases}$$

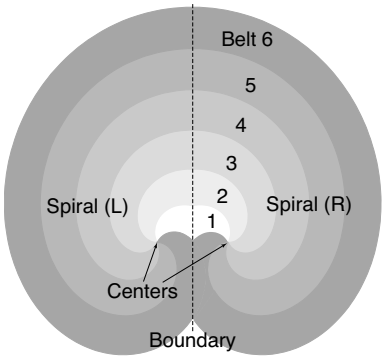

Figure 7: Two Archimedean spirals in the phase synchronization state when $d = 2a$ and $\Delta\varphi = \pi$.

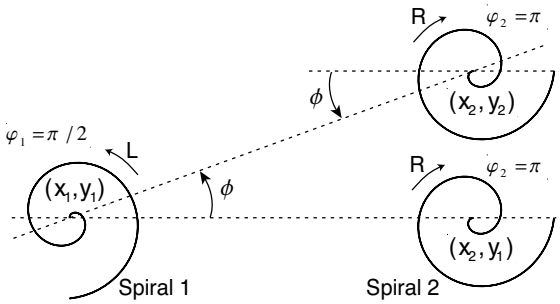

Figure 8: Phase difference depending on the relative positions of two centers.

By observing spiral 2 from spiral 1, on the other hand, the phase of spiral 2 (φ_2) advances by ϕ. Therefore, phase difference $\Delta\varphi$ after the movement can be written as

$$\Delta\varphi = (\varphi_2 + \phi) - (\varphi_1 - \phi) = \varphi_2 - \varphi_1 + 2\phi. \qquad (3)$$

If the rotation directions of spirals 1 and 2 are, respectively, R and L, $\Delta\varphi = \varphi_2 - \varphi_1 - 2\phi$.

We next consider the case where the rotation directions are the same. Suppose that spiral 2 in Fig. 8 rotates counterclockwise (L). Then, φ_2 decreases by ϕ by observing spiral 2 from spiral 1 after the movement; therefore, the phase difference does not change in this case. To sum up, the phase difference depends on the relative positions of two spirals only if their rotation directions are different.

Based on the above-mentioned dependence, we show how large the barrier is when the rotation directions of spirals 1 and 2 are L and R, respectively. Figure 9 shows the area of center (x_2, y_2) that satisfies $d \in S_d$ (S_d is given in Fig. 6(a)) when $\varphi_2 - \varphi_1 = \pi$ and $(x_1, y_1) = (0, 0)$. Note that in this case, distance d and phase difference $\Delta\varphi$ are written as $d = \sqrt{x_2^2 + y_2^2}$ and $\Delta\varphi = \pi + 2\tan^{-1}\frac{y_2}{x_2}$, respectively. From the figure, the barrier is deeply dented when $y = 0$. This unique shape

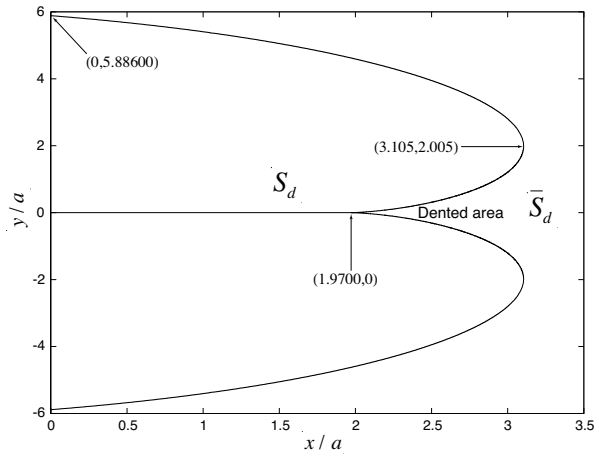

Figure 9: Barrier between two spirals when $\varphi_2 - \varphi_1 = \pi$ and center $(x_1, y_1) = (0, 0)$. The widths of the two spirals are a.

affects the pair decay rate, as discussed in the subsequent section.

Behavior after First Touch

Adjacent Species Violation

The adjacent species violation (ASV) indicates that a belt of species i touches a belt that is made up of species other than $i-1$, i, and $i+1$. If the phase synchronization hypothesis is true, ASV occurs only in two cases. (1) At the beginning of the CA model when newborn spirals touch one another for the first time. (2) When some spiral belts encounter one another after they invade an empty area created by a partial decay.

In the above-mentioned two cases, new spirals often appear. The following experiment clarifies the relationship between the appearance of new spirals and ASV. Two circles are used as the initial state of the CA model (see Fig. 10). Each circle is equally divided into six parts and each part is filled with molecules of the same species. The two circles become two spirals soon after the beginning of the CA model, they grow larger (i.e., their numbers of turns increase), and then they touch each other. The rotation directions of the two spirals and the phase difference between them can be determined *a priori* depending on how the six species are arranged on the 12 parts in the two circles. Figure 10 shows the initial state (the arrangement of species in the two circles and distance d_0 between their centers) and what happens after their first touch until $t = 3000$.

The following summarizes the experimental results shown in Fig. 10.

1. Without ASV ($\Delta\varphi = \pi$), no new spirals appear.
2. When ASV occurs ($\Delta\varphi = 0$) and two spirals are both L, one spiral deterministically appears with the R di-

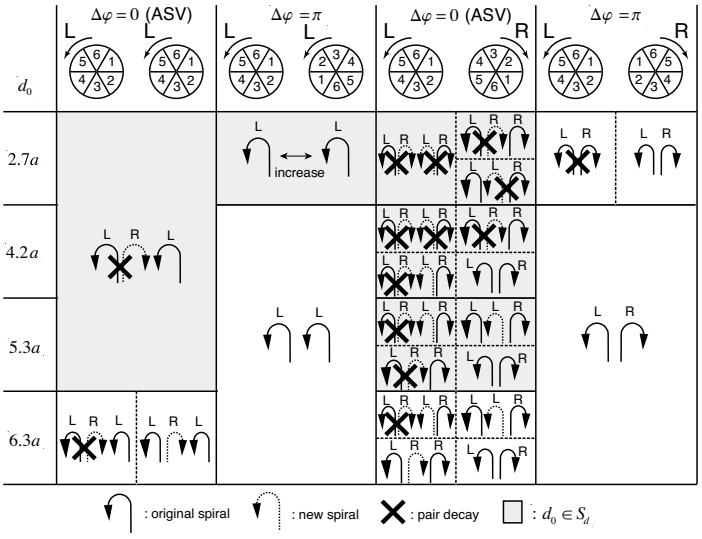

Figure 10: Relationship between ASV and the birth of new spirals. For clarity, we set $\gamma = 1$. The sample mean of width $a = 10.47$. ASV occurs when $\Delta\varphi = 0$.

rection. When $\Delta\varphi = 0$ and one spiral is L and the other is R, one of the following four cases happens: two new spirals with different directions, one new spiral with the L direction, one new spiral with the R direction, or no new spirals. Which of these cases occurs is random, even if the experiments are made under the same conditions excluding random numbers.

3. When the centers are inside the barrier ($d_0 \in S_d$), pair decay occurs with a high probability. If the directions are both L, the distance between the centers deterministically increases. Figures 12(j)–(l) illustrate the increase of the distance. In this case, the movement of the centers is not according to Brownian motion, but they repel each other perhaps to enter the phase synchronization state.

Emergence of New Spirals

We learned from the above experiments that ASV is a necessary condition for creating new spirals. Then, how does a new spiral emerge after ASV? From our observations, after belts of species i and j ($\neq i-1, i, i+1$) commit ASV, the molecules of species $i+1$ ($j+1$) in the belt of species j (i) begin to actively reproduce after touching the belt of species i (j), so that they form a small cluster of species $i+1$ ($j+1$) between the belts. (Note that a belt of species i includes a small number of molecules of species $i-1, i-2, \ldots$) The number of clusters increases as the two spirals rotate, and eventually the clusters form a spiral. Figures 12(g)-(i) show the generation process of a new spiral when $(\gamma, P_{\text{decay}}) = (1, 0.1)$. It takes about 100 time steps to create a new spiral.

Table 2: Pair decay rate r_p and probability $p_c(2.4a)$. r_p is measured over 200 experiments for $(c_0, P_{\text{decay}}) = (0.7, 0.06)$. $a = 11.69$

d_0	$2.0a$	$2.4a$	$2.7a$	$3.0a$	$3.4a$	$3.8a$
r_p	0.995	0.90	0.71	0.42	0.21	0.11
$p_c(2.4a)$	1.0	0.973	0.643	0.439	0271	0.169

Effect of Barrier on Pair Decay

Table 2 shows the occurrence rate (r_p) of pair decay, which is obtained by carrying out the same experiment as shown in Fig. 10 when $\Delta\varphi = \pi$ and the directions are L and R. From the table, the following two results are obtained. (1) A pair decay occurs almost deterministically when $d_0 = 2a$. (2) Rate r_p largely changes when d_0 is between $2.4a$ and $3.0a$. The above two results can be expressed in different words with the random walk of a center and the S_d barrier: a pair decay occurs at the inner part of the dented area in Fig. 9, and the probability that a center enters the inner part is sensitive to d_0 if d_0 is near the entrance of the dented area. By means of the random walk simulation, we obtain probability $p_c(\ell)$ that the shortest distance between two centers during a random walk is less than ℓ. Table 2 demonstrates that $p_c(2.4\text{a})$ approximates r_p.

Survivability Evaluation

In this section, we evaluate how long the hypercycle system can live depending on c_0 and P_{decay}. Here, the death of the system means that the concentration of at least one species is zero. Figure 11 shows average life spans for various c_0 and P_{decay} pairs. From the figure, we can see that a system can live long if P_{decay} is a little larger than that on the boundary between the S and Q regions in parameter space (c_0, P_{decay}), where we assume that the S region in Fig. 4 still exists even under the Q2 region as a long and very narrow region.

We explain this result as follows. In order for the system to live long, forming a spiral is definitely required. Experiments verify that hypercycle systems cannot live long if spiral structures are completely broken at each time step without changing the concentrations of each species. Namely, the system's death comes soon after the number of spirals becomes zero. As shown in Fig. 5, compared with the S region, the Q region has an advantage since the number of spirals in the region may increase (due to ASV after a partial decay). A large P_{decay} value increases not only the frequency of partial decays, but also the frequency of complete decays; therefore, there is an optimal P_{decay} value for each c_0, which is a little larger than P_{decay} on the boundary.

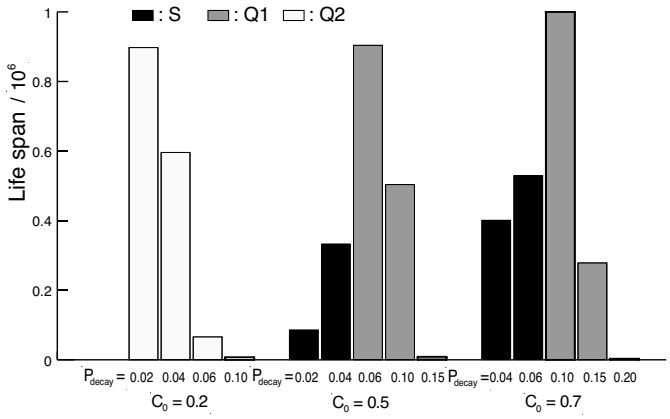

Figure 11: The life span of a hypercycle system averaged over ten trials. For all trials, the execution of CA stops at $t = 10^6$ time steps.

Discussion

A hypercycle system consists of two levels of dynamical systems: species (low-level systems) and spirals (high-level systems). One significant result of our study is that although the stability of low-level systems has an effect on the behavior of high-level systems (Fig. 4), the survivability of the hypercycle system (Fig. 11) can be explained only by interactions among high-level systems. The stability analysis of a hypercycle system based only on the dynamics of the concentrations (or numbers) of low-level systems, which does not take into account the high-level system, may lead to different conclusions from those in this paper.

Our results also suggest that the fitness of a species in a hypercyclic organization depends not only on its stability and its efficiency of reproduction, but also on the interactions of high-level systems; furthermore, an increase in the stability of high-level systems does not always result in an increase in the fitness. Although all of our results are experimental, some of them may be theoretically derived, for example, by solving the Ginzburg-Landau equation (Gabbay, Ott, & Guzdar 1998).

Conclusions

We have analytically and experimentally described the behavior of hypercycle spirals in the two-dimensional CA model. The following summarizes our main results:

- A spiral can be approximated by an Archimedean spiral and the center, width, and phase of the spiral change according to Brownian motion.
- From the phase synchronization hypothesis, there is a barrier that does not allow two spirals to come close to each other. Pair decay occurs at the inner part of a dented area of the barrier with a high probability.
- Computational experiments indicate that adjacent species violation (ASV) is a necessary condition for creating new spirals.
- Parameter space $(c_0, P_{\mathrm{decay}})$ consists of three regions. A hypercycle system can live long if P_{decay} is a little larger than that on the boundary between the S and Q regions.

From the above results, the survivability of a hypercycle system can be explained based on the birth and death process of spirals. In order for the system to live long, the spirals in the system should be somewhat unstable, since new spirals cannot emerge when existing spirals are too stable. The stability of spirals can be controlled by the stability (P_{decay}) of molecular species. If the amount of components used for building up molecules (c_0) increases, it is necessary that the molecules be slightly more unstable for the hypercycle system to live long.

Acknowledgements

This work was supported by the Telecommunications Advancement Organization of Japan.

References

Altmeyer, S.; Wilke, C.; and Martinetz, T. 1998. How fast do structures emerge in hypercycle-systems? In *GWAL*.

Boerlijst, M. C., and Hogeweg, P. 1991. Spiral wave structure in pre-biotic evolution: Hypercycles stable against parasites. *Physica D* 48:17–28.

Boerlijst, M. C., and Hogeweg, P. 1992. Self-structuring and selection: Spiral waves as a substrate for prebiotic evolution. In *Artificial Life II*, 255–276.

Cronhjort, M., and Blomberg, C. 1996. Chasing: A mechanism for resistance against parasites in self-replicating systems. In *Artificial Life IV*, 413–417.

Eigen, M., and Schuster, P. 1979. *The Hypercycle, A Principle of Natural Selforganization.* Berlin: Springer-Verlag.

Eigen, M. 1971. Self-organization of matter and the evolution of biological macro-molecules. *Naturwissenschaften* 58:465–523.

Gabbay, M.; Ott, E.; and Guzdar, P. N. 1998. Reconnection of vortex filaments in the complex Ginzburg-Landau equation. *Physical Review E* 58:2576–2579.

Gebinoga, M. 1995. Hypercycles in biological systems. In *Endocytobiology VI*, 263–276.

Hofbauer, J., and Sigmund, K. 1988. *The Theory of Evolution and Dynamical Systems.* Cambridge Univ. Press.

Vespalcova, Z.; Holden, A. V.; and Brindley, J. 1995. The effect of inhibitory connection in a hypercycle: a study of the spatio-temporal evolution. *Physics Letters A* 197:147–156.

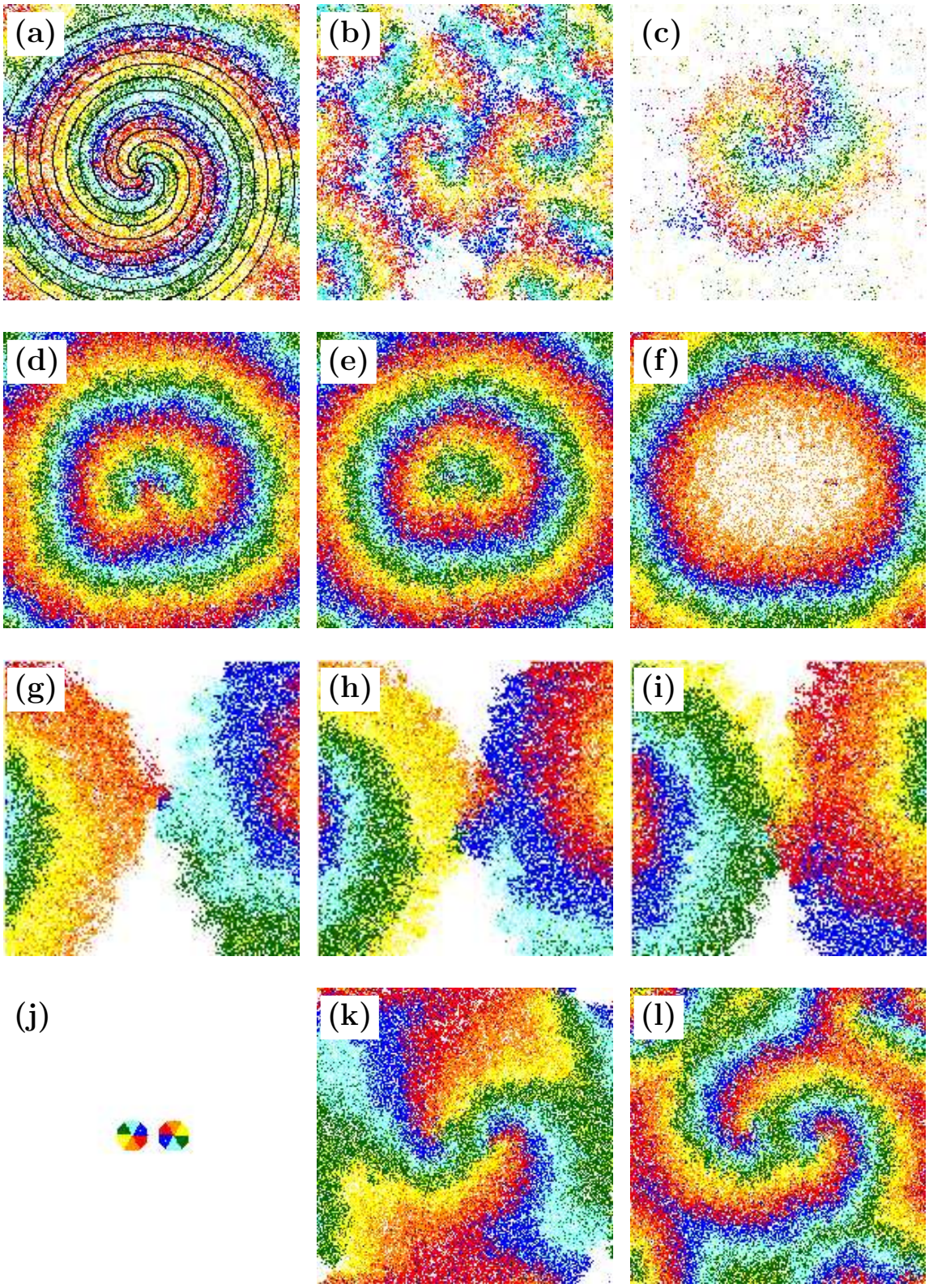

Figure 12: Spiral patterns on a 200×200 CA lattice. (a) Identification by an Archimedean spiral. $(c_0, P_{\text{decay}}) = (1, 0.12)$. (b) Empty areas existing between spirals in the Q1 region. $(c_0, P_{\text{decay}}) = (0.7, 0.1)$. (c) Spirals in the Q2 region surrounded by empty cells. $(c_0, P_{\text{decay}}) = (0.2, 0.04)$. (d)–(f) Pair decays in progress. $t = 2070, 2450, 2650$. (g)–(i) Emergence of new spirals between two spirals. $t = 390, 420, 450$. (j)–(l) Two spirals repelling each other. $t = 0, 450, 850$.